Molecular interaction of the antiviral compound CW-33 and its analogues with the NS2B-NS3 protease of the Japanese encephalitis virus

KUAN-CHUNG CHEN[1], YU-FONG LIN[2], AN-CHENG HUANG[3], JING-YANG GAO[1], CHENG-WEN LIN[2,4] and JIN-CHERNG LIEN[1,5]

[1]School of Pharmacy, [2]Department of Medical Laboratory Science and Biotechnology, China Medical University, Taichung 40402; [3]Department of Nursing, St. Mary's Junior College of Medicine, Nursing and Management, Yilan 26647; [4]Department of Biotechnology, Asia University, Taichung 41354; [5]Department of Medical Research, Hospital of China Medical University, Taichung 40402, Taiwan, R.O.C.

Received September 27, 2018; Accepted February 7, 2019

DOI: 10.3892/ijmm.2019.4113

Abstract. In a previous study from our group, a novel compound, namely CW-33 (ethyl 2-(3',5'-dimethylanilino)-4-oxo-4,5-dihydrofuran-3-carboxylate) was identified that exhibited antiviral activity for Japanese encephalitis virus (JEV). The viral NS2B-NS3 serine protease serves an important role in cytoplasmic cleavage events that occur during viral polyprotein maturation. The inhibition of viral RNA and protein syntheses was responsible for the antiviral activities of the novel furanonaphthoquinone derivatives that were discovered for the prevention of JEV infection. Consequently, the present study examined the molecular docking simulation of JEV protease with compound CW-33 and its analogues, and developed quantitative structure-activity relationship (QSAR) models to assess the potential antiviral activities of these compounds with regard to JEV. Molecular docking simulation indicated the potential ligand-protein interactions associated with the antiviral activities of these compounds. According to the results of the QSAR models, the secondary amine group was an important moiety required for compound bioactivity, which enabled the formation of hydrogen bonding with the residue Glu155. Furthermore, the aromatic ring mapping of the phenyl moiety of each compound was predicted to form a π-cation interaction with residue Arg76, whereas the hydrophobic feature represented by the ethyl moiety exhibited hydrophobic contacts with residue Glu74. Finally, the hydrophobic substituents in the meta-position of the phenyl ring further contributed to the efficacy of the antiviral activity. These results unravel the structural characteristics that are required for binding of CW-33 to the JEV protease and can be used for potential therapeutic and drug development purposes for JEV.

Correspondence to: Professor Jin-Cherng Lien, School of Pharmacy, China Medical University, 91 Hsueh-Shih Road, Taichung 40402, Taiwan, R.O.C.
E-mail: jclien@mail.cmu.edu.tw

Professor Cheng-Wen Lin, Department of Medical Laboratory Science and Biotechnology, China Medical University, 91 Hsueh-Shih Road, Taichung 40402, Taiwan, R.O.C.
E-mail: cwlin@mail.cmu.edu.tw

Abbreviations: JEV, Japanese encephalitis virus; NS, non-structural; QSAR, quantitative structure-activity relationship; CoMFA, comparative force field analysis; CoMSIA, comparative similarity indices analysis; H-bond, hydrogen bond; E-state, electrotopological state; MLR, multiple linear regression; SVM, support vector machine; CHARMM, Chemistry at Harvard Macromolecular Mechanics; PLS, partial least-squares

Key words: Japanese encephalitis virus, molecular docking simulation, pharmacophore features, quantitative structure-activity relationship models

Introduction

Japanese B encephalitis is a severe central nervous system disorder caused by an arbovirus called Japanese encephalitis virus (JEV) (1,2). JEV belongs to the *Flaviviridae* family and is maintained in a zoonotic cycle with domestic pigs and wild birds serving as reservoirs for viral propagation. In addition, mosquitoes such as *Culex tritaeniorhynchus*, *Culex vishnui*, *Culex gelidus*, *Culex fuscocephala*, *Culex annulirostris*, *Anopheles peditaeniatus* (Leicester), *Anopheles barbirostris van der Wulp*, and *Anopheles subpictus* can serve as vectors of JEV (3-6). This virus has a single-stranded, positive-sense RNA genome with an open reading frame encoding for three structural proteins, namely precursor proteins to membrane and envelope components, capsid proteins and seven non-structural (NS) proteins (7).

Several different vaccines are currently available for the prevention of Japanese B encephalitis caused by JEV (8-15), although no specific chemotherapeutic agents exist for this disease (16,17), which disproportionately targets young people. Therefore, the identification of a drug candidate for

Japanese B encephalitis is an important research field for the development of promising antiviral therapeutics. Previous studies have demonstrated that the novel compound CW-33 (ethyl 2-(3',5'-dimethylanilino)-4-oxo-4,5-dihydrofuran-3-carboxylate; compound 01 in Fig. 1) exhibits antiviral activity with regard to the enteroviral A71 and the JEV T1P1 strains (18-20). The present study aimed to further examine the development of the compound CW-33 as a drug candidate for the prevention of infection by the JEV strain T1P1.

Computer-aided drug design can increase the odds of developing suitable lead candidates by identifying key features of compounds required for future drug development, whereas it can concomitantly accelerate the process of drug development. In the present study, the compound CW-33 and its analogues were investigated *in silico* using docking simulation and quantitative structure-activity relationship (QSAR) models. Their antiviral activities for JEV were then evaluated. The antiviral activities of the furanonaphthoquinone derivatives with regard to JEV are ascribed to the inhibition of the viral RNA and the viral protein syntheses (21). The viral NS2B-NS3 serine protease has an important role in cytoplasmic cleavage events that occur during the viral polyprotein maturation, and it is responsible for cleaving the viral polyprotein at the NS2A/NS2B, NS2B/NS3, NS3/NS4A, and NS4B/NS5 junctions (22). Molecular docking simulation of JEV protease with compound CW-33 and its analogues was performed to investigate the ligand-protein interaction network responsible for the antiviral activities of these compounds. A ligand-based approach was further applied and the two dimensional (2D)-QSAR models were developed to determine the representative molecular descriptors related to the antiviral activities. Finally, the following analyses were performed: Pharmacophore modeling, comparative force field analysis (CoMFA), and comparative similarity index analysis (CoMSIA). These processes aimed to develop models for the investigation of the common pharmacophore features and to identify the relationship between five physicochemical properties of these compounds and their corresponding antiviral activities.

Materials and methods

Data collection. The X-ray crystal structure of the JEV protease was downloaded from the RCSB Protein Data Bank with PDB ID 4R8T (23). The Prepare protein protocol in the discovery studio 2.5 (DS2.5) was employed to remove crystal waters in the crystal structure. Furthermore, this software was used for the repair of incomplete residues and the protonation of the JEV protease structure that was performed with the Chemistry at Harvard Macromolecular Mechanics (CHARMM) force field (24). This force field was able to optimize the side-chain conformation of repaired residues. The binding site of the JEV protease was defined from the protein cavities that were close to the active site residues of the JEV protease and was expanded to the volume of 288.375 $Å^3$.

The compound CW-33 and its analogues were obtained from the Lien laboratory (School of Pharmacy, China Medical University, Taichung, Taiwan) (18-20) (Fig. 1 and Table I). All the 15 compounds were drawn using ChemBioOffice 2010 (Perkin Elmer, Waltham, MA, USA), and prepared by the Prepare Ligand protocol in DS2.5 to modify their ionization state according to the physiological ionization setting. The efficacy of the antiviral activities of the 15 compounds was determined using the cytopathic effect assay for JEV (18,20).

Table I. pIC_{50} values of CW-33 and its analogues with regard to the viral cytopathic effect assay against the JEV strain T1P1.

Compound	R^1	R^2	R^3	pIC_{50}
01 (CW-33)	-	-	-	5.09
02	-H	-H	-F	4.98
03	-H	-F	-H	<3.00
04	-F	-H	-H	3.94
05	-H	-H	-OMe	4.18
06	-H	-OMe	-H	3.90
07	-OMe	-H	-H	<3.00
08	-H	-H	-Cl	4.30
09	-H	-Cl	-H	3.26
10	-Cl	-H	-H	<3.00
11	-H	-H	-Br	5.49
12	-H	-Br	-H	5.51
13	-Br	-H	-H	5.70
14	-H	-Me	-H	3.94
15	-H	-Et	-H	3.91

pIC_{50}, -log half maximal inhibitory concentration; JEV, Japanese encephalitis virus.

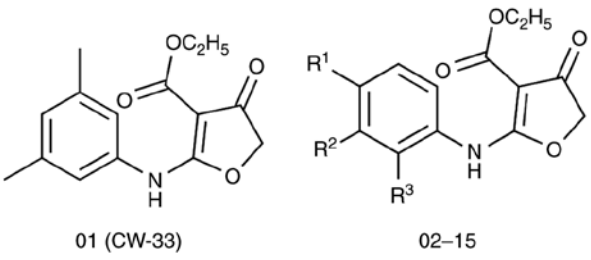

Figure 1. Chemical scaffolds of CW-33 and its analogues.

Molecular docking simulation. The LigandFit protocol (25) in DS 2.5 was employed to simulate the docking poses of each compound using a shape filter and the Monte-Carlo ligand conformation generation (24). Subsequently, the poses were optionally minimized with the CHARMM force field (24). Similar docking poses were filtered using the clustering algorithm. Four different scoring functions were employed to evaluate the docking poses -PLP1 (26), -PLP2 (27), -PMF (28), and the Dock score. The scoring functions, -PLP1, -PLP2, and -PMF, were evaluated by the sum of the two types of the pairwise interaction, namely H-bond and steric interactions, between the protein and the compound. The scoring function of the Dock score was based on a force field approximation as follows:

Dock score = -(ligand\receptor interaction energy+ligand internal energy)

Table II. Experimental and predicted pIC_{50} values obtained by MLR and SVM models, and scoring functions of each complex obtained by docking simulations.

		pIC_{50} (predicted)		Scoring functions			
Compound	pIC_{50}	MLR	SVM	-PLP1	-PLP2	-PMF	Dock score
01 (CW-33)	5.09	4.41	4.16	76.15	72.63	46.27	42.021
02	4.98	4.94	4.92	74.48	68.18	37.99	40.49
03[a]	<3.00	4.07	4.25	74.35	61.59	46.23	40.434
04	3.94	3.81	4.00	74.34	68.52	36.51	40.272
05	4.18	4.49	4.21	64.87	60.85	51.62	42.795
06[a]	3.90	3.87	3.89	71.82	61.05	56.84	43.857
07[a]	<3.00	3.81	3.86	79.60	65.39	55.74	40.432
08	4.30	4.37	4.24	67.56	60.28	52.07	42.201
09	3.26	3.34	3.78	72.47	68.86	47.92	44.907
10[a]	<3.00	3.43	3.79	77.32	61.04	44.41	42.746
11	5.49	5.77	5.55	77.94	63.42	56.86	44.851
12[a]	5.51	5.34	5.48	68.4	61.67	50.66	46.429
13	5.70	5.37	5.50	67.39	55.68	46.28	44.888
14	3.94	3.97	4.00	68.83	61.38	51.23	46.782
15	3.91	4.32	4.10	79.14	74.3	46.57	40.94

[a]Test set. pIC_{50}, -log half maximal inhibitory concentration; MLR, multiple linear regression; SVM, support vector machine.

The LigPlot+ program (29) was employed to generate the 2D ligand-protein interaction diagrams.

2D-QSAR models. The 2D-QSAR models were developed by multiple linear regression (MLR) and support vector machine (SVM) using MATLAB (MathWorks, Natick, MA, USA) and LibSVM (National Taiwan University) (30), respectively. All 15 compounds displayed in Table II were classified as the training set (10 compounds) and the test set (5 compounds) with their pIC_{50} values (-log IC_{50}, given in terms of molar concentration). The genetic function approximation protocol (31) in DS2.5 was employed to determine the suitable molecular descriptors for the prediction models.

Pharmacophore model. The 3D (three dimensional)-QSAR pharmacophore generation protocol in DS2.5 was employed to generate a pharmacophore model using the catalyst hypoGen algorithm (32). Low-energy conformations were generated for each compound by the FAST generation protocol. The common pharmacophore model was then constructed by a list of four different pharmacophore features, namely H-bond donor, H-bond acceptor, hydrophobic, and aromatic ring interactions.

CoMFA and CoMSIA models. CoMFA (33) and CoMSIA (34) were employed with all 15 compounds to construct 3D-QSAR models by SYBYL-X (Certara, Princeton, NJ, USA). CoMFA was employed to evaluate the steric and electrostatic field descriptors with the distance-dependent dielectric method using Lennard-Jones and Coulombic potential energies, respectively. CoMSIA was used to evaluate five physico-chemical properties, namely steric, electrostatic, hydrophobic, H-bond donor, and H-bond acceptor, with a Gaussian function based on the distance. The partial least-squares (PLS) regression was used to obtain a linear correlation between the biological activity values and the properties of CoMFA and CoMSIA.

Results and Discussion

In earlier studies, scientists have indicated that the NS2B/NS3 protease may be a suitable target for antiviral compounds (35). In addition, a compound obtained from a secondary metabolite of *Boesenbergia pandurata* (Schult.) has been noted for its potential antiviral activity and possible docking pose towards the JEV NS2B/NS3 protease (36). In the present study, molecular docking simulation of JEV protease was performed to investigate the ligand-protein interaction network responsible for the antiviral activities, as well as QSAR models to determine the representative molecular descriptors and common pharmacophore features.

Molecular docking simulation. The chemical structures of compound CW-33 and its analogues are displayed in Fig. 1 and Table I. IC_{50} refers to the half maximal inhibitory concentration. The results of the docking simulations with regard to the JEV protease and the compound CW-33 and its analogues, are reported in Table II with their corresponding scoring values. Fig. 2 displays the docking poses of compounds 03, 07, 10, 11. The docking poses of compounds 03, 07, 10, which had pIC_{50} <3 revealed that the amine group was rotated. This caused an alignment of the phenyl substituents of the para-moiety of compounds 03, 07, 10 with the meta-moiety of the phenyl substituents of compound 11. The alignment indicated that the meta-substituent of the phenyl ring may be

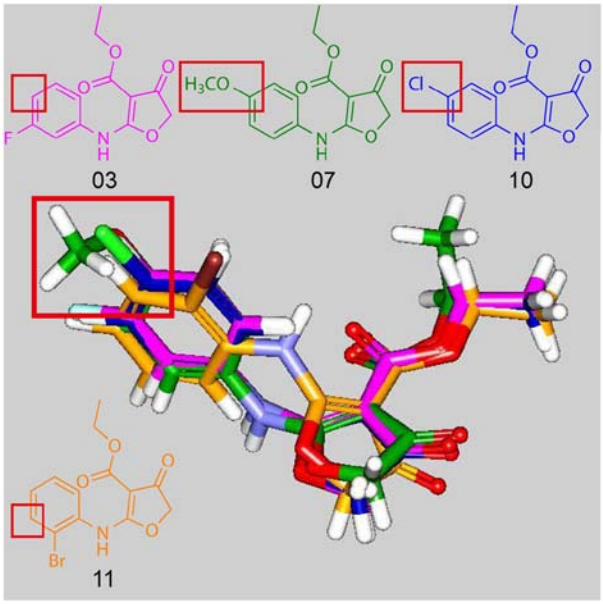

Figure 2. Compounds 03, 07, 10, 11 superimposed by their docking poses.

more suitable for the design of active CW-33 derivatives. The docking poses of the three compounds that exhibited optimal biological activities, i.e. compounds 01, 09, 15, are displayed in Fig. 3. The amine group of these compounds contained hydrogen bonds (H-bonds) with the residues Asn152 and Glu155, while the phenyl group established a π-cation interaction with residue Arg76. In addition, all of the compounds exhibited hydrophobic contacts with residues Glu74, Arg76, Trp83, Ile147, Gly148, Asn152, Gly153, Val154, and Glu155. Finally, compounds 01 and 15 formed additional hydrophobic contacts with residues Phe85, Asp86, Arg87, and Leu149 due to the presence of methyl or ethyl groups. These interactions that were either hydrogen bonding or hydrophobic contacts, were responsible for compound stabilization in the binding site of the enzyme.

2D-QSAR models. The genetic function approximation protocol resulted in the identification of three representative descriptors, namely ES_Sum_ssNH, molecular_weight, and Jurs_WNSA_2 that were used to construct the 2D-QSAR models. The ES_Sum_ssNH descriptor is an electrotopological state (E-state) descriptor (37,38), which denotes the E-state of the NH group with two single bonds. It implies that the secondary amine group is one of the most important moieties related to bioactivity. The molecular_weight descriptor is the sum of the atomic masses of the compounds under investigation. The Jurs_WNSA_2 descriptor refers to the surface-weighted partial surface areas obtained by multiplying the atomic charge-weighted positive surface area by the total molecular solvent-accessible surface area and dividing it by a factor of 1,000.

The MLR model was constructed with a training set of 10 compounds using the 3 representative descriptors described above. The following linear equation was obtained:

pIC_{50} = 15.0708-6.7849*ES_Sum_ssNH + 0.0671*Molecular_Weight + 0.0588*Jurs_WNSA_2

The SVM model was constructed using the same training set and representative descriptors. The test set of 5 compounds was employed to validate the accuracy of the prediction of both 2D-QSAR models. The predicted pIC_{50} values obtained by MLR and SVM models are listed in Table II. Fig. 4 illustrates the correlations between predicted pIC_{50} and experimental pIC_{50} in the MLR and SVM models. The square correlation coefficients (R^2) of the training set were 0.8339 and 0.7901, respectively. Both models predicted favorable bioactivities for CW-33 and its analogues with the exception of compounds 03, 07, and 10, which exhibited pIC_{50} values <3. The data implied that the poor bioactivities of compounds 03, 07, and 10 were not associated with these three representative descriptors. However, the three representative descriptors were associated with the antiviral activities with regard to the JEV protease.

Pharmacophore model. The present study aimed to investigate the common pharmacophore features based on the 3D structures of all 15 compounds. The results of the best pharmacophore hypothesis are illustrated in Fig. 5A with the pharmacophore features. The pharmacophore model included two H-bond acceptor features, one aromatic ring feature, and one hydrophobic feature. The mapping of the pharmacophore features onto compounds 01 and 15 suggested that the oxygen atoms of the carboxylate and the 4-oxo-4,5-dihydrofuran moieties matched the H-bond acceptors features. The ethyl moiety matched the hydrophobic feature and the phenyl moiety matched the aromatic ring feature (Fig. 5B and C). This was in line with the results of the docking simulation, suggesting that the phenyl moiety of each compound exhibited a π-cation interaction with residue Arg76. In addition, the oxygen atoms of the carboxylate moiety formed H-bonds with residue Asn152, and the ethyl moiety exhibited hydrophobic contacts with residue Glu74.

CoMFA and CoMSIA models. To determine the correlation between the efficacy of antiviral activity and the compound functional groups, the CoMFA and CoMSIA models were constructed using all 15 compounds that were aligned to the pharmacophore model described above. Following PLS analysis, the CoMFA model with three components exhibited significant steric fields (100% contribution), whereas the CoMSIA model with four components indicated significant steric, hydrophobic, and H-bond donor fields (15.9, 63.2 and 20.9% contribution, respectively). The predicted pIC_{50} values for the two significant CoMFA and CoMSIA models are listed in Table III. The correlations between predicted pIC_{50} vs. experimental pIC_{50} values for the two models are displayed in Fig. 6. The square correlation coefficients (R^2) were 0.7607 and 0.8234, respectively. The pIC_{50} values of compounds 03, 07 and 10 were >3, indicating that the CoMFA and CoMSIA models could partially predict the estimation of this endpoint. Compound 03 exhibited predicted pIC_{50} values of 2.72 and 2.58 in the CoMFA and CoMSIA models, respectively. Compound 07 exhibited a predicted pIC_{50} value of 2.80 in the CoMSIA model, and compound 10 demonstrated a predicted pIC_{50} value of 2.78 in the CoMFA model. The data derived by these two models may explain the poor antiviral efficacy of compounds 03, 07, and 10 and may predict their corresponding pIC_{50}.

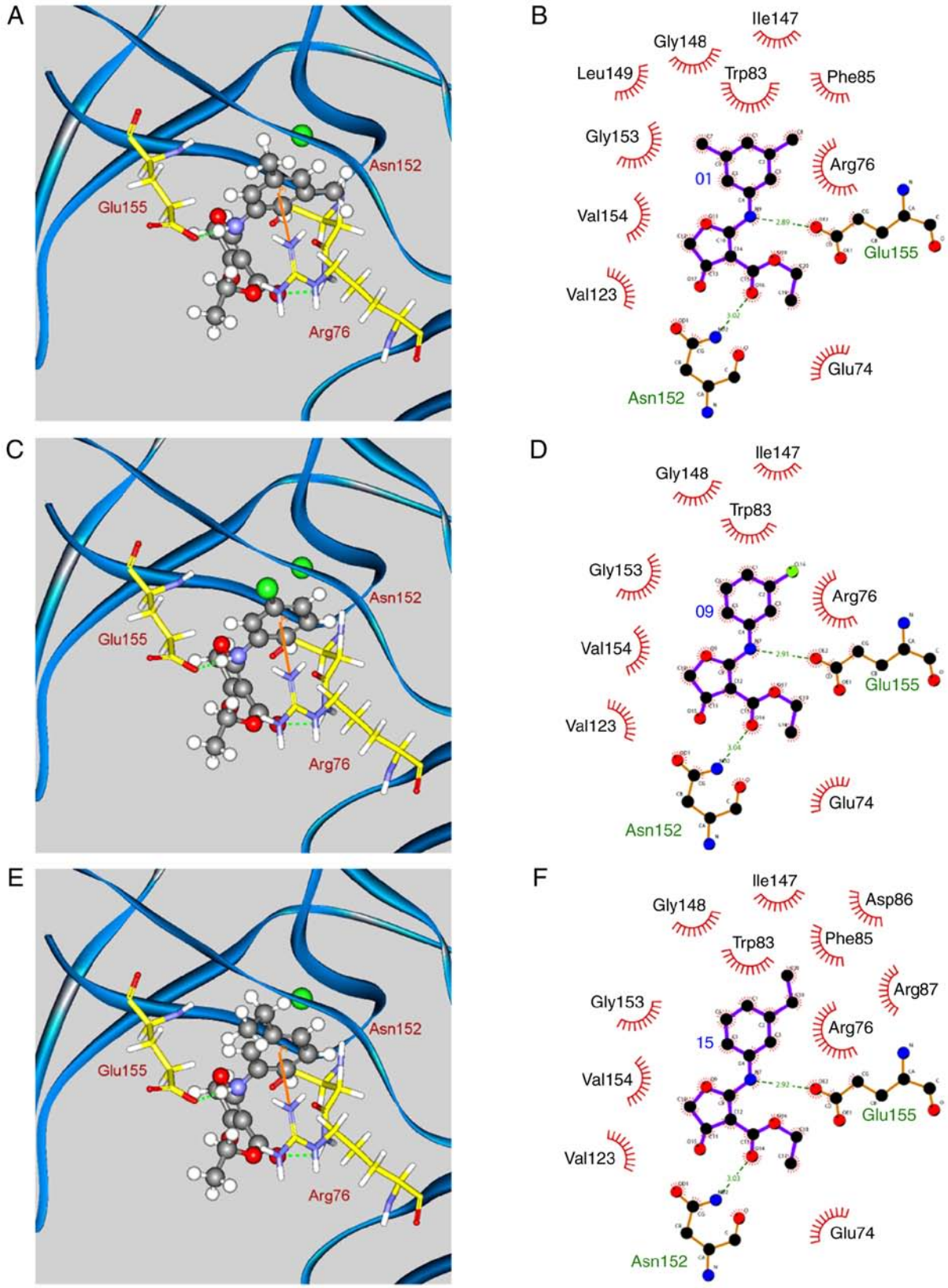

Figure 3. Docking poses of compounds (A and B) 01, (C and D) 09 and (E and F) 15 in the binding site of the JEV protease. The right panels were drawn with the LigPlot+ program. JEV, Japanese encephalitis virus.

Fig. 7 illustrates the CoMFA and CoMSIA contour maps for compound CW33, with the favorable and unfavorable regions (80 and 20%, respectively) using SD*coefficients for each field.

Since CW-33 and its analogues have similar chemical structures, we focused on the contour maps of the phenyl moiety of CW-33. In the CoMFA model, the results indicated that the favored steric fields were in close proximity to the

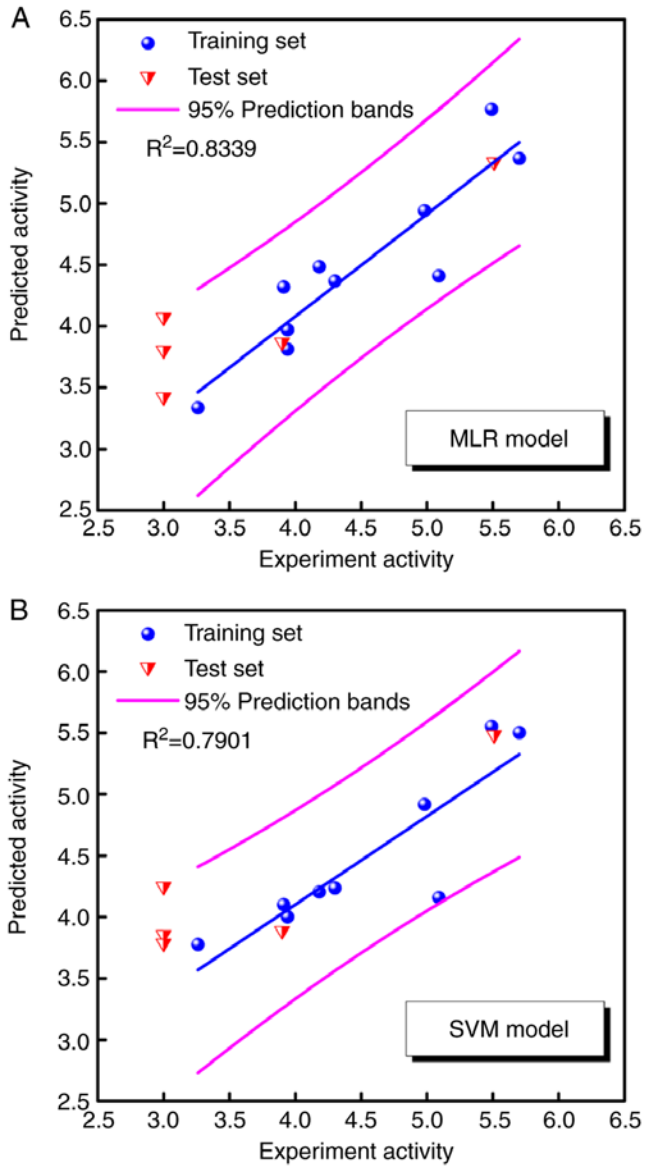

Figure 4. Correlation between predicted pIC_{50} values and experimental pIC_{50} values for the (A) MLR and (B) SVM models. pIC_{50}, -log half maximal inhibitory concentration; MLR, multiple linear regression; SVM, support vector machine.

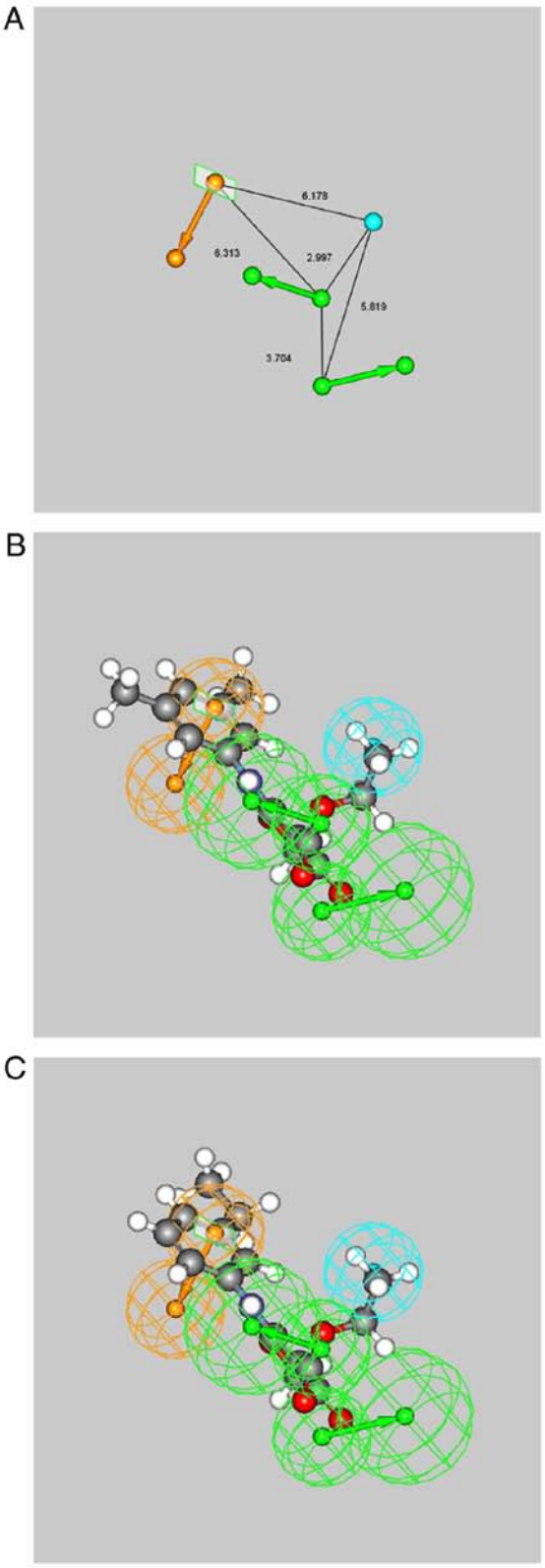

Figure 5. (A) Pharmacophore features and mapping of compounds (B) 01 and (C) 15. The hydrogen bond acceptor features are illustrated by the green lines, the hydrophobic features are illustrated by the light blue ball and the aromatic ring features are illustrated by the orange line.

meta-moieties of the phenyl substituents, whereas the disfavored steric fields were in close proximity to the para-moieties of the phenyl substituents (Fig. 7A). Specific favored steric fields were identified close to the meta- and ortho-moieties of the phenyl substituents in the CoMSIA model (Fig. 7B). The data further indicated that the hydrophobic substituents that were beneficial to the bioactivity were found in the meta- and para-positions of the phenyl ring (Fig. 7C). In contrast to the hydrophobic sites, the current model did not provide information regarding the regions responsible for H-bonding residing in close proximity to the phenyl moiety of CW-33 (Fig. 7D). In line with the results of docking simulation, the data implied that the hydrophobic substituents in the meta- and ortho-positions of the phenyl rings were beneficial to the potency of the antiviral compounds.

In an earlier study, there was no suitable 3D structure of NS2B protease, so the authors built the 3D model of NS2B protein using homology modelling (36). In the present study, the X-ray crystal structure of the JEV protease was employed from the RCSB Protein Data Bank to increase the precision of docking simulation. The current results indicated that the

Table III. Experimental and predicted pIC_{50} values obtained by CoMFA and CoMSIA models.

Compound	pIC_{50}	pIC_{50} (predicted)	
		CoMFA	CoMSIA
01 (CW-33)	5.09	4.73	4.57
02	4.98	5.01	4.68
03	<3.00	2.72	2.58
04	3.94	4.71	4.41
05	4.18	4.47	4.40
06	3.90	3.75	3.66
07	<3.00	3.67	2.80
08	4.30	4.78	4.65
09	3.26	3.36	3.31
10	<3.00	2.78	3.74
11	5.49	4.93	5.07
12	5.51	5.37	5.60
13	5.70	4.81	5.24
14	3.94	4.39	4.13
15	3.91	3.74	4.37

pIC_{50}, -log half maximal inhibitory concentration; CoMFA, comparative force field analysis; CoMSIA, comparative similarity indices analysis.

residues Glu155, Arg76, and Glu74 have important roles in the docking of compounds. In case that these key residues are mutant, homology modelling can be used to generate a reliable mutant type JEV protease for docking simulation to indicate that some compounds may change their docking poses to interact with other residues, while others may fail in docking. However, the effects of mutation in their bioactivities should still be confirmed by *in vitro* and *in vivo* experimental studies.

As previous studies have indicated that the compound CW-33 and its analogues exhibit antiviral activity with regard to the JEV T1P1 strain, this study aimed to indicate the key features of compounds which may be related to their antiviral activities. The results provided some beneficial suggestions for further studies of synthesis of CW-33 analogues on JEV therapeutics. Because the compounds employed to perform the QSAR models in the present study were obtained from previous studies and the compound CW-33 and its analogues have similar main scaffolds, these QSAR models would be not suitable for compounds which have very different chemical scaffold than compound CW-33. Additionally, the docking poses of compounds in the domain of JEV protease indicated the suitable docking poses and interactions with JEV protease and provided some beneficial suggestions to increase the binding interactions between compounds and JEV protease. However, the docking simulation cannot be used to evaluate the antiviral activities of compounds, so it will be necessary to perform *in vivo* or *in vitro* experiments to evaluate the antiviral activities of compounds which are synthesised in further studies.

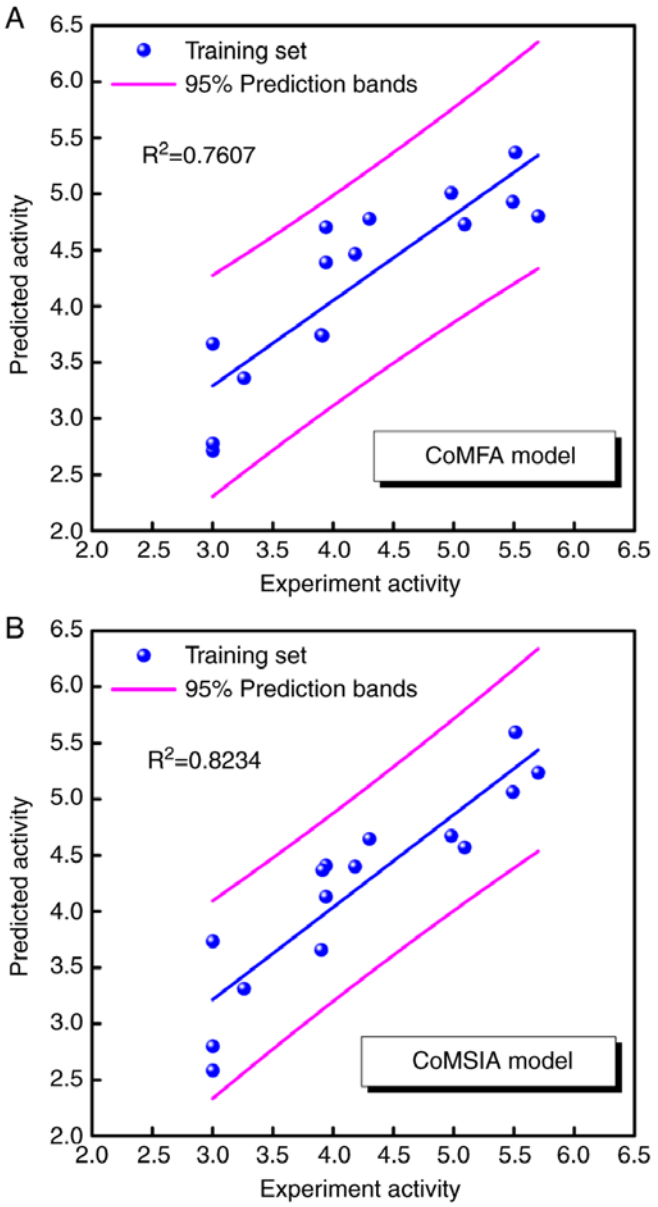

Figure 6. Correlation between predicted and experimental pIC_{50} values for (A) the CoMFA and (B) CoMSIA models. pIC_{50}, -log half maximal inhibitory concentration; CoMFA, comparative force field analysis; CoMSIA, comparative similarity indices analysis.

As suggested by docking simulation and 2D-QSAR models, the secondary amine group is a significant moiety required for antiviral bioactivity that can form H-bonds with residue Glu155. The sum of the atomic masses and the charged surface-weighted partial surface areas were also related to the antiviral activities of the compounds towards JEV. The pharmacophore model further suggested that the aromatic ring features in the phenyl moieties of each compound formed π-cation interactions with residue Arg76. In addition, the H-bond acceptor features were notably the oxygen atoms of the carboxylate moiety that could form a H-bond with residue Asn152. The hydrophobic feature of the ethyl moiety exhibited hydrophobic contacts with residues Glu74. The CoMFA and CoMSIA models indicated that the hydrophobic substituents in the meta-moieties of the phenyl rings were beneficial for the antiviral activity of the compounds investigated. The results

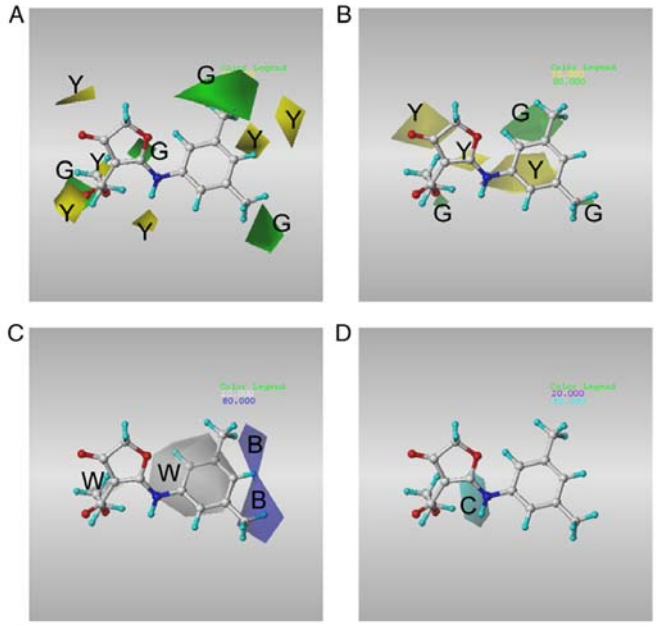

Figure 7. Contour plots illustrating (A) steric properties as demonstrated by the CoMFA model and (B) steric, (C) hydrophobic, and (D) hydrogen bond donor properties as determined by the CoMSIA model. CW-33 is shown as a template. CoMFA, comparative force field analysis; CoMSIA, comparative similarity indices analysis B, blue; C, cyan; G, green; W, white; Y, yellow.

offer important insight that can be used for further studies on JEV therapeutics.

Acknowledgements

Not applicable.

Funding

This study was supported by the China Medical University (grant no. CMU107-S-33), the Ministry of Science and Technology of Taiwan (grant nos. MOST 105-2320-B-039-032, MOST 106-2320-B-039-011 and MOST 107-2320-B-039-058) and by the China Medical University Hospital (grant nos. DMR-107-135, DMR-107-136, DMR-108-108 and DMR-108-142).

Availability of data and materials

All data generated or analyzed during the present study are included in this published article.

Authors' contributions

KCC, ACH, JYG, CWL and JCL conceived and designed the experiments, performed the experiments, analyzed the data and wrote the paper. YFL and CWL performed the cytopathic effect assay, determined the efficacy of antiviral activity and calculated the IC_{50} values. All authors read and approved the final manuscript.

Ethics approval and consent to participate

Not applicable.

Patient consent for publication

Not applicable.

Competing interests

CWL, ACH and JCL have produced patents on CW-33.

References

1. Unni SK, Růžek D, Chhatbar C, Mishra R, Johri MK and Singh SK: Japanese encephalitis virus: From genome to infectome. Microbes Infect 13: 312-321, 2011.
2. Simon LV and Kruse B: Encephalitis, Japanese. In: StatPearls. StatPearls Publishing, Treasure Island, FL, 2017.
3. van den Hurk AF, Ritchie SA and Mackenzie JS: Ecology and geographical expansion of Japanese encephalitis virus. Annu Rev Entomol 54: 17-35, 2009.
4. Karunaratne SH and Hemingway J: Insecticide resistance spectra and resistance mechanisms in populations of Japanese encephalitis vector mosquitoes, *Culex tritaeniorhynchus* and Cx. *gelidus*, in Sri Lanka. Med Vet Entomol 14: 430-436, 2000.
5. Thenmozhi V, Rajendran R, Ayanar K, Manavalan R and Tyagi BK: Long-term study of Japanese encephalitis virus infection in *Anopheles subpictus* in Cuddalore district, Tamil Nadu, South India. Trop Med Int Health 11: 288-293, 2006.
6. Kumar K, Arshad SS, Selvarajah GT, Abu J, Toung OP, Abba Y, Bande F, Yasmin AR, Sharma R, Ong BL, *et al*: Prevalence and risk factors of Japanese encephalitis virus (JEV) in livestock and companion animal in high-risk areas in Malaysia. Trop Anim Health Prod 50: 741-752, 2018.
7. Solomon T, Ni H, Beasley DW, Ekkelenkamp M, Cardosa MJ and Barrett AD: Origin and evolution of Japanese encephalitis virus in southeast Asia. J Virol 77: 3091-3098, 2003.
8. Schiøler KL, Samuel M and Wai KL: Vaccines for preventing Japanese encephalitis. Cochrane Database Syst Rev: CD004263, 2007.
9. Turtle L and Driver C: Risk assessment for Japanese encephalitis vaccination. Hum Vaccin Immunother 14: 213-217, 2018.
10. Jelinek T, Burchard GD, Dieckmann S, Bühler S, Paulke-Korinek M, Nothdurft HD, Reisinger E, Ahmed K, Bosse D, Meyer S, *et al*: Short-term immunogenicity and safety of an accelerated pre-exposure prophylaxis regimen with Japanese encephalitis vaccine in combination with a rabies vaccine: A phase III, multicenter, observer-blind study. J Travel Med 22: 225-231, 2015.
11. Singh A, Mitra M, Sampath G, Venugopal P, Rao JV, Krishnamurthy B, Gupta MK, Sri Krishna S, Sudhakar B, Rao NB, *et al*: A Japanese encephalitis vaccine from India induces durable and cross-protective immunity against temporally and spatially wide-ranging global field strains. J Infect Dis 212: 715-725, 2015.
12. Vu TD, Nguyen QD, Tran HTA, Bosch-Castells V, Zocchetti C and Houillon G: Immunogenicity and safety of a single dose of a live attenuated Japanese encephalitis chimeric virus vaccine in Vietnam: A single-arm, single-center study. Int J Infect Dis 66: 137-142, 2018.
13. Fan YC, Lin JW, Liao SY, Chen JM, Chen YY, Chiu HC, Shih CC, Chen CM, Chang RY, King CC, *et al*: Virulence of Japanese encephalitis virus genotypes I and III, Taiwan. Emerg Infect Dis 23: 1883-1886, 2017.
14. Connor B and Bunn WB: The changing epidemiology of Japanese encephalitis and New data: The implications for new recommendations for Japanese encephalitis vaccine. Trop Dis Travel Med Vaccines 3: 14, 2017.
15. Ginsburg AS, Meghani A, Halstead SB and Yaich M: Use of the live attenuated Japanese Encephalitis vaccine SA 14-14-2 in children: A review of safety and tolerability studies. Hum Vaccin Immunother 13: 2222-2231, 2017.
16. Solomon T, Dung NM, Kneen R, Gainsborough M, Vaughn DW and Khanh VT: Japanese encephalitis. J Neurol Neurosurg Psychiatry 68: 405-415, 2000.
17. Hegde NR and Gore MM: Japanese encephalitis vaccines: Immunogenicity, protective efficacy, effectiveness, and impact on the burden of disease. Hum Vaccin Immunother 13: 1-18, 2017.

18. Huang SH, Lien JC, Chen CJ, Liu YC, Wang CY, Ping CF, Lin YF, Huang AC and Lin CW: Antiviral activity of a novel compound CW-33 against Japanese encephalitis virus through inhibiting intracellular calcium overload. Int J Mol Sci 17: E1386, 2016.
19. Wang CY, Huang AC, Hour MJ, Huang SH, Kung SH, Chen CH, Chen IC, Chang YS, Lien JC and Lin CW: Antiviral potential of a novel compound CW-33 against enterovirus A71 via inhibition of viral 2A protease. Viruses 7: 3155-3171, 2015.
20. Lien JC, Wang CY, Lai HC, Lu CY, Lin YF, Gao GY, Chen KC, Huang AC, Huang SH and Lin CW: Structure analysis and antiviral activity of CW-33 analogues against Japanese encephalitis virus. Sci Rep 8: 16595, 2018.
21. Takegami T, Simamura E, Hirai K and Koyama J: Inhibitory effect of furanonaphthoquinone derivatives on the replication of Japanese encephalitis virus. Antiviral Res 37: 37-45, 1998.
22. Bera AK, Kuhn RJ and Smith JL: Functional characterization of cis and trans activity of the Flavivirus NS2B-NS3 protease. J Biol Chem 282: 12883-12892, 2007.
23. Weinert T, Olieric V, Waltersperger S, Panepucci E, Chen L, Zhang H, Zhou D, Rose J, Ebihara A, Kuramitsu S, *et al*: Fast native-SAD phasing for routine macromolecular structure determination. Nat Methods 12: 131-133, 2015.
24. Brooks BR, Bruccoleri RE, Olafson BD, States DJ, Swaminathan S and Karplus M: CHARMM: A program for macromolecular energy minimization and dynamics calculations. J Comput Chem 4: 187-217, 1983.
25. Venkatachalam CM, Jiang X, Oldfield T and Waldman M: LigandFit: A novel method for the shape-directed rapid docking of ligands to protein active sites. J Mol Graph Model 21: 289-307, 2003.
26. Gehlhaar DK, Verkhivker GM, Rejto PA, Sherman CJ, Fogel DB, Fogel LJ and Freer ST: Molecular recognition of the inhibitor Ag-1343 by Hiv-1 protease: Conformationally flexible docking by evolutionary programming. Chem Biol 2: 317-324, 1995.
27. Gehlhaar DK, Bouzida D and Rejto Paul A: Reduced dimensionality in ligand-protein structure prediction: Covalent inhibitors of serine proteases and design of site-directed combinatorial libraries. In: Rational Drug Design American Chemical Society, pp 292-311, 1999.
28. Muegge I and Martin YC: A general and fast scoring function for protein-ligand interactions: A simplified potential approach. J Med Chem 42: 791-804, 1999.
29. Laskowski RA and Swindells MB: LigPlot+: Multiple ligand-protein interaction diagrams for drug discovery. J Chem Inf Model 51: 2778-2786, 2011.
30. Fan RE, Chen PH and Lin CJ: Working set selection using second order information for training support vector machines. J Mach Learn Res 6: 1889-1918, 2005.
31. Rogers D and Hopfinger AJ: Application of genetic function approximation to quantitative structure-activity relationships and quantitative structure-property relationships. J Chem Inf Comput Sci 34: 854, 1994.
32. Li H, Sutter J and Hoffman R: HypoGen: An automated system for generating 3D predictive pharmacophore models. In: Pharmacophore Perception, Development and Use in Drug Design. Guner O (ed). International University Line, La Jolla, 2000.
33. Cramer RD, Patterson DE and Bunce JD: Comparative molecular field analysis (CoMFA). 1. Effect of shape on binding of steroids to carrier proteins. J Am Chem Soc 110: 5959-5967, 1988.
34. Klebe G, Abraham U and Mietzner T: Molecular similarity indices in a comparative analysis (CoMSIA) of drug molecules to correlate and predict their biological activity. J Med Chem 37: 4130-4146, 1994.
35. Yang CC, Hsieh YC, Lee SJ, Wu SH, Liao CL, Tsao CH, Chao YS, Chern JH, Wu CP and Yueh A: Novel dengue virus-specific NS2B/NS3 protease inhibitor, BP2109, discovered by a high-throughput screening assay. Antimicrob Agents Chemother 55: 229-238, 2011.
36. Seniya C, Mishra H, Yadav A, Sagar N, Chaturvedi B, Uchadia K and Wadhwa G: Antiviral potential of 4-hydroxypanduratin A, secondary metabolite of Fingerroot, *Boesenbergia pandurata* (Schult.), towards Japanese Encephalitis virus NS2B/NS3 protease. Bioinformation 9: 54-60, 2013.
37. Hall LH, Mohney B and Kier LB: The electrotopological state: Structure information at the atomic level for molecular graphs. J Chem Inf Comput Sci 31: 76-82, 1991.
38. Hall LH and Kier LB: The E-state as the basis for molecular structure space definition and structure similarity. J Chem Inf Comput Sci 40: 784-791, 2000.